Available online at www.sciencedirect.com
ScienceDirect
Journal of the European Ceramic Society 30 (2010) 3389–3396
www.elsevier.com/locate/jeurceramsoc

Control of pore channel size during freeze casting of porous YSZ ceramics with unidirectionally aligned channels using different freezing temperatures

Liangfa Hu [a], Chang-An Wang [a,*], Yong Huang [a], Chencheng Sun [b], Sheng Lu [b], Zijun Hu [b]

[a] State Key Lab of New Ceramics and Fine Processing, Department of Materials Science and Engineering, Tsinghua University, Beijing 100084, PR China
[b] National Key Lab of Advanced Functional Composite Materials, Aerospace Research Institute of Materials & Processing Technology, Beijing 100076, PR China

Received 12 April 2010; received in revised form 4 July 2010; accepted 19 July 2010
Available online 21 August 2010

Abstract

Porous yttria-stabilized zirconia (YSZ) ceramics with unidirectionally aligned pore channels were prepared by freezing YSZ/tert-butyl alcohol (TBA) slurry under different freezing temperatures of −30, −78 and −196 °C, respectively. After removing the frozen TBA *via* freeze-drying in vacuum at −50 °C, the green samples were sintered at 1450 °C for 2 h in air. The results showed that the freezing temperature significantly influenced microstructure and properties of the porous YSZ ceramics. Both microstructure observation and pore size distribution indicated that the pore channel size decreased significantly with decreasing freezing temperature, regardless of microstructure variations in the individual sample. Both porosity and room-temperature thermal conductivity of the porous YSZ ceramics varied under different freezing temperatures. Regardless of microstructure variations in the samples under different freezing temperatures, all samples had unidirectional pore channels with increasing pore channel size along the freezing direction. The fabricated samples had remarkably low thermal conductivities both in directions perpendicular and parallel to the channel direction, thus rendering them suitable for applications in thermal insulations.

Keywords: Freezing casting; Porosity; Thermal conductivity; Yttria-stabilized zirconia; Insulators

1. Introduction

Porous ceramics is a field of intense research for their wide applications in catalyst carrier, ceramic filter, sensor, porous electrode, biomaterials, thermal barrier, and so on.[1,2] Various fabrication methods of porous ceramics have been performed, including the pore-foaming technique, infiltration of ceramic sol into template structures, gel-casting, slip-casting, starch consolidation, microwave processing, electrophoretic deposition, and freeze casting.[3–9] As a novel method, freeze casting has many advantages, including a small processing shrinkage, controllable and wide porosity range, high strength, and so forth.[10–14] Fukasawa et al.[12,13] applied freeze casting to fabricate porous alumina and silicon nitride ceramics with unidirectionally aligned pore channels. Deville et al.[10] fabricated hydroxyapatite ceramics with lamellar and cellar pores, and the as-prepared porous ceramics exhibited high compressive strength.

The unidirectional solidification of freezing vehicles in the ceramic slurry, under a certain freezing temperature, forms a channeled structure and pushes the ceramic particles into spaces between adjacent frozen channels. After freeze-drying, a porous ceramic structure remains with pores in the size and shape of the prior ice prism. The control of pore structure would be very important because of its relation to properties. Many factors, including the composition and solid loading of slurry as well as sintering conditions, influence the microstructure and properties of porous ceramics fabricated by the freeze casting. For example, Han et al.[15] adopted a camphene-based freeze casting method to fabricate ceramics with aligned, equiaxed pores, in which the pore volume fraction, channel size and pore shape were controlled by varying freezing temperature, solid content and sintering condition. Yoon et al.[16] fabricated macroporous alumina ceramics with aligned microporous walls by unidirectionally freezing foamed aqueous ceramic suspensions. The size of the macropores was controlled by adjusting the stirring

* Corresponding author. Tel.: +86 10 62785488; fax: +86 10 62785488.
E-mail addresses: wangca@tsinghua.edu.cn, huliangfa@gmail.com (C.-A. Wang).

0955-2219/$ – see front matter © 2010 Elsevier Ltd. All rights reserved.
doi:10.1016/j.jeurceramsoc.2010.07.032

speed during the foaming process. Hong et al.[17] produced highly porous zirconia ceramic bodies with interconnected pores by freeze casting technique using camphene-based slurries. The pore volume fraction and pore size were controllable by adjusting the initial solid content in the mixed slurries. Zuo et al.[18] fabricated porous hydroxyapatite (HAP) ceramics with different morphologies by the freeze casting method. The morphologies of HAP ceramics were modified by adjusting the concentration of polyvinyl alcohol (PVA) additive in the HAP slurries. Nevertheless, more attention should be placed on the effect of freezing temperature on the microstructure and properties of porous ceramics. Because the freezing temperature also exerts impact on solidification behavior of freezing vehicles and thus the pore structure left by the frozen vehicles.

In the present work, a processing route, using different freezing temperatures during freeze casting, to control the pore channel size in porous YSZ ceramics with unidirectionally aligned pore channels was reported. The as-fabricated samples were characterized by observing the microstructure and evaluating pore size, pore size distribution, porosity and the room-temperature thermal conductivity. The unidirectionally aligned pore channels produced by this method offered distinct applications of porous YSZ ceramics in thermal insulators: one end with high porosity along the channel direction was promising in thermal insulation, and the other end which was much denser provided high strength for load bearing.

2. Experiment procedure

2.1. Sample preparation

Commercially available YSZ powder (ZrO_2–8 mol% Y_2O_3, AR grade, Fanmeiya Powders Co. Ltd., Jiangxi, China) was used as the starting material. This YSZ powder has a median size (d_{50}) of 1.26 μm (d_{10} = 0.44 μm, and d_{90} = 3.23 μm) and a specific surface area of 6.49 m^2/g. Tert-butyl alcohol (TBA, chemical purity, Beijing Yili Chemical Co., Beijing, China) and polyvinyl butyral (PVB) were used as the shaping vehicle and the binder in the freeze casting process, respectively.

Cylindrical polyamide mold, with an outside diameter of 78 mm, an inside diameter of 26 mm and a height of 30 mm, was glued on a copper plate of 5 mm thickness using silicon gel. The copper plate was immersed in the freezing agents, i.e., chilled alcohol (CAH) with temperature of −30 °C, solidified carbon dioxide (SCD) with temperature of −78 °C and liquid nitrogen (LN2) with temperature of −196 °C. The top of the mold was open so that the upper surface of the slurry was exposed to the atmosphere at room temperature of 25 °C.

A premixed solution was prepared by mixing 0.5 wt% PVB into TBA. YSZ powder (15 vol%) was mixed with the premixed solution (85 vol%) and ball-milled for 4 h to generate a homogeneous suspension. To adjust the suspension to a proper flowability during casting, a selected alkali solution was added into the slurry. The slurry was then poured into the mold and subjected to unidirectionally freezing using different freezing agents. After freezing, the frozen bodies were freeze-dried in vacuum at −50 °C using a freeze-dryer (Type FD-1A-50, Boyikang Corp., Beijing, China). Cylindrical green compacts with a height of 18 mm and a diameter of 25 mm were then produced and carefully removed from the molds. Subsequently, the green compacts were sintered at 1450 °C for 2 h in air.

2.2. Characterization

Microstructure was observed using a scanning electron microscope (SEM, JSM 6700F, JEOL, Tokyo, Japan) on certain parts of the sample with different distance from the cooled plate (3 mm, 9 mm and 15 mm). In particular, in order to observe the pore channel size and microstructure of the section paralleled to the cooled plate, the samples were infiltrated with ethylene-vinyl acetate (EVA) copolymer to avoid breaking and make it more adaptive to the working condition. Thereafter, the samples were ground and analyzed using SEM. Pore channel size was determined by measuring the size of pore channels from the microstructure of the section paralleled to the cooled plate. The microstructure was taken at four randomly-selected locations on each sample (two samples per condition). Pore size distribution was analyzed by a mercury intrusion porosimetry (AutoPore-IV9510, Micromeritics Instrument Corp., United States) on certain parts of the sample with different distance from the cooled plate (3 mm, 9 mm and 15 mm). Bulk density of the sintered samples was measured from sample mass and dimension, and relative density thus porosity were determined from the ratio of the measured bulk density to the theoretical one of the YSZ material, which was taken as 6.0 g/cm^3. Three samples were used to determine the average porosity. Thermal conductivity at room temperature was measured on 5 mm × 5 mm × 3 mm machined specimens, using a Thermal Transport Option (TTO) of Physical Properties Measurement System (PPMS, Model 6000, Quantum Design, United States). The TTO system measured thermal conductivity λ by applying heat from the heater shoe in order to create a user-specified temperature differential (ΔT) between the two thermometer shoes, which were connected to the two sides of sample using epoxies (including silver-filled H20E and nonconductive tra-bond 816H01). TTO dynamically modeled the thermal response of the sample to the low-frequency, square-wave heat pulse, thus expediting data acquisition. TTO then calculated thermal conductivity directly from the applied heat power, resulting ΔT, and sample geometry.

3. Results and discussion

3.1. Formation of porous structure

Freeze casting of YSZ/TBA slurry was employed to produce porous YSZ ceramics with unidirectionally pore channels using different freezing temperatures, which were offered by different freezing agents of CAH, SCD and LN2. Fig. 1 shows the schematical illustration of freeze casting system and pore structure formation during freeze casting. The system mainly consists of the TBA ice prism, the ceramic walls and the liquid particle suspension. This method exploits the fact that TBA

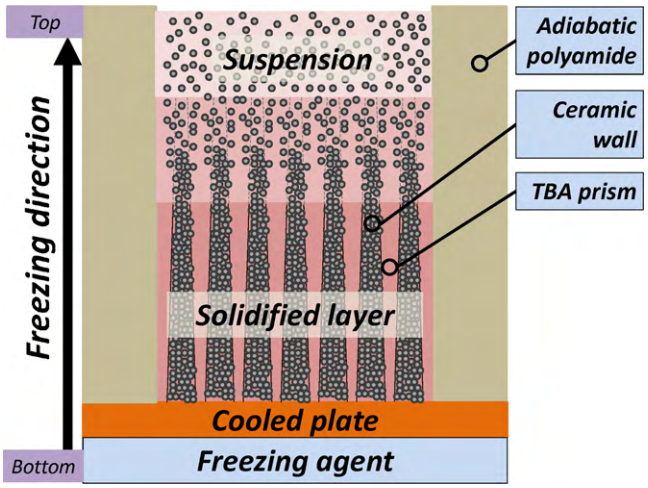

Fig. 1. Schematical illustration of freeze casting system and pore structure formation during freeze casting.

normally forms long straight ice prisms without any branches when solidified under a certain freezing temperature.[19] During freeze casting, TBA gradually crystallized to form unidirectionally aligned ice prisms parallel to the freezing direction, running from low temperature of the bottom to high temperature of the top. Meanwhile, the ceramic particles were repelled by the growing TBA ice prisms, and bound by PVB, to cohere together and form strong pore channel walls. Typically within 30–60 min, the solidification was complete, yielding a solid green compact. The green compact was then demolded and placed in vacuum at −50 °C for 24 h to allow the sublimation of TBA. Solid TBA could be easily converted to the gaseous state, because the saturated vapor pressure of TBA (8–10 kPa) is high enough to allow sublimation in vacuum. The unidirectionally aligned TBA crystals sublimed and then left one-dimensional channeled pores.

Notably, the pore channels tended to align with increasing pore channel size in the freezing direction, regardless of the change of pore channel size under different freezing temperatures. Owing to the thermal resistance of the solidified layer, the solidification velocity decreased with increasing layer thickness and caused an increase of prism spacing and thus pore channel size.

Fig. 2 shows the typical microstructure of the porous YSZ ceramics with unidirectionally aligned pore channels fabricated by freeze casting. The architectures in the sintered samples were observed along the different directions perpendicular, parallel and at a 45° angle to the cooled plate, as shown in Fig. 2(a)–(c), respectively. The perpendicular section to the cooled plate clearly indicated that growth of the close-packed TBA crystals, upon unidirectionally freezing, incorporated the ceramic particles and binders together between adjacent TBA ice prisms. Subsequent high-vacuum sublimation of the TBA ice produced well-ordered micro-channeled structures parallel to the freezing direction (Figs. 1 and 2(a)). Moreover, both the parallel section and the section at the 45° angle to the cooled plate indicated that the ceramic walls were regularly arranged between the adjacent pore channels which showed a hexagonal cross-section (Fig. 2(b) and (c)). The channeled architectures with pore channel size around 100 μm and wall thickness ranging from 30 to 100 μm were observed in the section at the 45° angle to the cooled plate (Fig. 2(c)). High-magnification image showed

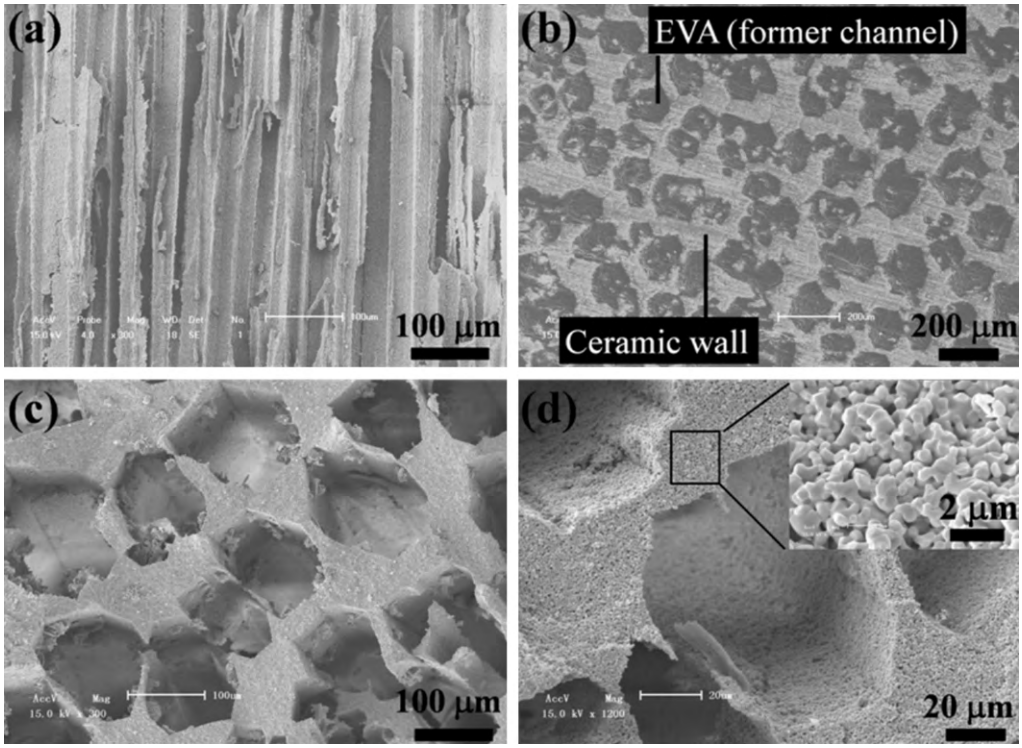

Fig. 2. Typical SEM micrographs of porous YSZ ceramics with unidirectionally aligned pore channels: (a) perpendicular section to the cooled plate, (b) parallel section to cooled plate (prepared by EVA infiltration), (c) section with a 45° angle to the cooled plate and (d) high-magnification micrographs.

Table 1
Variations of pore channel size with distance from the cooled plate in porous YSZ ceramics with unidirectionally aligned pore channels under different freezing temperatures of −30, −78 and −196 °C.

Freezing agent	Freezing temperature (°C)	Distance from the cooled plate (mm)	Pore size (μm)
CAH	−30	3	31.6 ± 14.6
		9	51.8 ± 17.3
		15	80.4 ± 21.6
SCD	−78	3	28.1 ± 4.5
		9	49.1 ± 14.2
		15	69.4 ± 18.6
LN2	−196	3	16.4 ± 3.9
		9	26.3 ± 7.5
		15	37.8 ± 5.7

submicrometer sized pores on the porous wall (Fig. 2(d)), which was supported by pore size distribution (Fig. 5).

The authors believe that the hexagonal cross-section of pore channels resulted from the crystallization characteristics of TBA. Among three crystalline phases of TBA which were noted by Oetting[20], phase II was reported to be stable below 8 °C, and phase II was found to transform into either phase I at 13 °C or phase III at 8 °C; the latter was reported to be stable between approximately 9 and 22 °C.[21] In other words, the phase II of TBA was the stable phase that existed in all the three kinds of green samples in the present work. Furthermore, McGregor et al.[22] pointed out that phase II of TBA contained three symmetry-independent molecules and these formed six-membered rings or hexamers with six hydrogen bonds forming each ring, as shown in Fig. 3. Fig. 3 also presented the crystal packing of these hexamers, which resulted in the hexagonal cross-section of pore channels formed by sublimation of TBA.

3.2. Microstructure

Fig. 4 shows the microstructure of unidirectionally aligned pore channels in the porous YSZ ceramics at different locations from the cooled plate of 15 mm (A1, B1 and C1), 9 mm (A2, B2 and C2), 3 mm (A3, B3 and C3) and under different

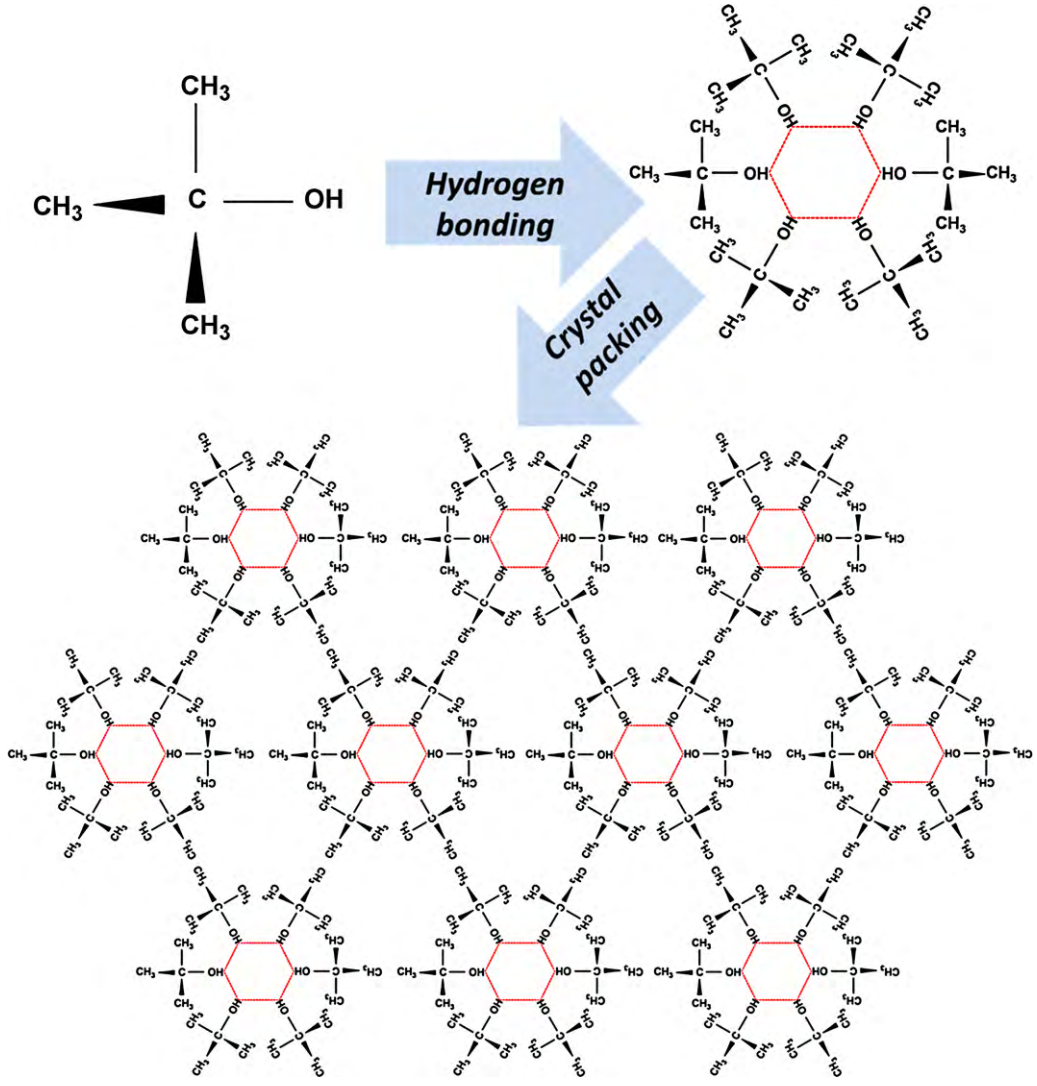

Fig. 3. Schematical illustration of TBA crystallization showing hexamers forming and hexagonal crystal packing.

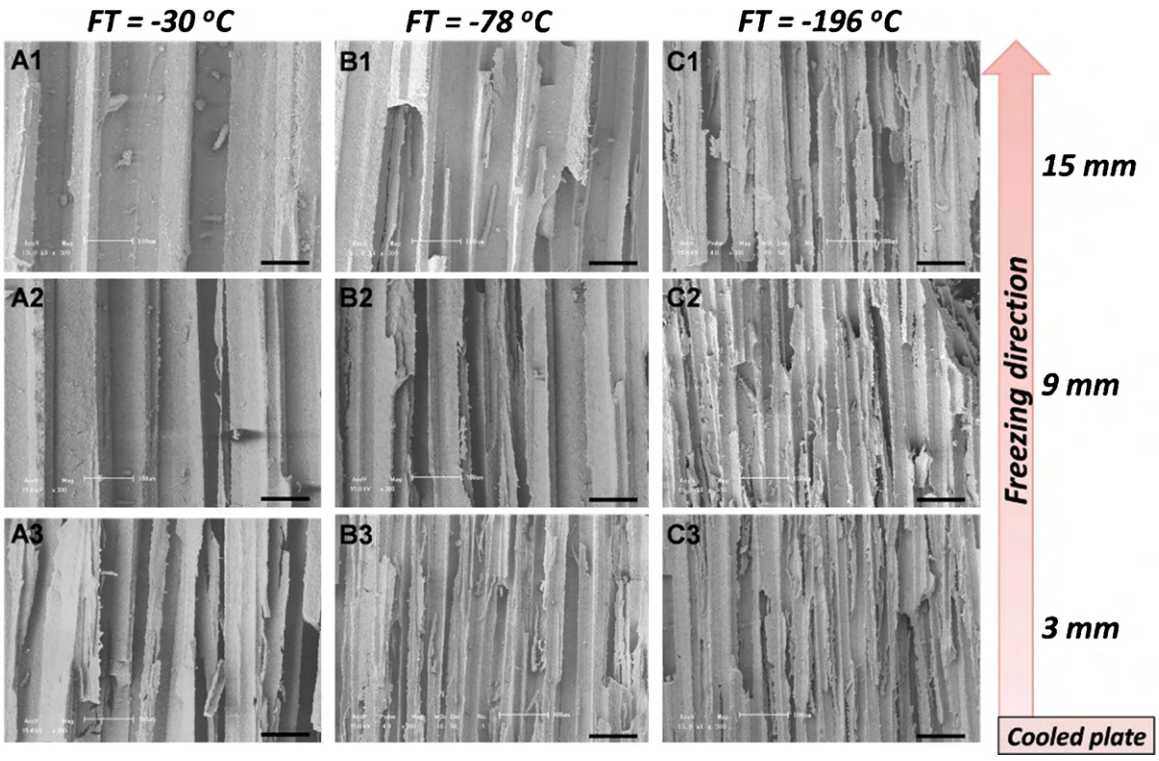

Fig. 4. Microstructure of unidirectionally aligned pore channels in the porous YSZ ceramics at different locations from the cooled end of 15 mm (A1, B1 and C1), 9 mm (A2, B2 and C2), 3 mm (A3, B3 and C3) and under different freezing temperatures of −30 °C (A1, A2 and A3), −78 °C (B1, B2 and B3) and −196 °C (C1, C2 and C3). FT: freezing temperature.

freezing temperatures of −30 °C (A1, A2 and A3), −78 °C (B1, B2 and B3) and −196 °C (C1, C2 and C3). It was observed that pore channel size decreased significantly with decreasing freezing temperature, regardless of the microstructure details in the individual samples. The authors believe that the solidification velocity increased with decreasing freezing temperature, and caused decreasing prism spacing and thus pore channel size. Moreover, the SEM micrographs also showed that the pore channels tended to align with increasing pore channel size from the cooled plate to the top of the mold, at a given freezing temperature. The possible reasons had been discussed above in the demonstration of pore structure formation in Fig. 1.

Table 1 shows the variations of pore channel size with distance from the cooled plate in porous YSZ ceramics with unidirectionally aligned pore channels under different freezing temperatures of −30, −78 and −196 °C. Pore channel size was determined by measuring the size of pore channels from the microstructure of the section paralleled to the cooled plate. The microstructure was taken at four randomly-selected locations on each sample (two samples per condition). Samples under lower freezing temperature revealed both lager pore channel size and broader size range. The pore channel size decreased with decreasing freezing temperature, regardless of the locations. The pore channel size at 3, 9 and 15 mm away from the cooled plate in samples under freezing temperature of −30 °C was 31.6, 51.8 and 80.4 μm, respectively. With decreasing freezing temperature, the corresponding values in samples under freezing temperature of −196 °C decreased to be 16.4, 26.3 and 37.8 μm, respectively. Regardless of freezing temperature, the pore channels size increased with distance away from the cooled plate. The results were consistent with microstructure development observation, as shown in Fig. 4.

Fig. 5 shows the pore size distribution (bold line) and cumulative pore volume of porous YSZ ceramics at different locations from the cooled plate of 15 mm (A1, B1 and C1), 9 mm (A2, B2 and C2), 3 mm (A3, B3 and C3) and under different freezing temperatures of −30 °C (A1, A2 and A3), −78 °C (B1, B2 and B3) and −196 °C (C1, C2 and C3). Pore size distribution was analyzed by a mercury intrusion porosimetry on certain parts of the sample with different distance from the cooled plate (3 mm, 9 mm and 15 mm). Each case presented a bimodal pore size distribution with peak locations at 0.35 and 14–72 μm, respectively. All pore distribution peaks revealed a narrow half-peak width, signifying a narrow pore size distribution. One peak had a fixed pore size of 0.35 μm at all locations and freezing temperatures. These pores were resulted from both burn-out of binders and grain packing in the ceramic walls, as shown in Fig. 2(d). The other peak was located in the range of larger sizes of 14–72 μm. These pores dominated over 90% of the cumulative pore volume in all samples, indicated by the cumulative pore volume curves (Fig. 5). They represented the unidirectionally aligned pore channels. The pore size varied significantly with freezing temperatures and locations: at a given location, the pore size decreased with decreasing freezing temperature; while at a given freezing temperature, the pore size increased with increasing distance away from the cooled plate. For example, the pore channel size at the location 15 mm away from the cooled plate of the samples decreased from 72

to 23 μm as the freezing temperature decreased from −30 to −196 °C; the pore channel size in the samples under the freezing temperature of −76 °C increased from 22 to 60 μm as the distance from cooled plate increased from 3 to 15 mm. The results were in agreement with microstructure observation, as shown in Fig. 4.

3.3. Porosity

Fig. 6 shows the variation of porosity with distance from the cooled plate in porous YSZ ceramics with unidirectionally aligned pore channels under different freezing temperatures of −30, −78 and −196 °C. The porosity decreased with decreasing freezing temperature, regardless of the locations. The porosity at locations 3, 9 and 15 mm away from the cooled plate in samples under freezing temperature of −30 °C was 76.7, 77.4 and 77.9%, respectively. With decreasing freezing temperature, the corresponding values in samples under freezing temperature of −196 °C decreased to be 73.1, 74.5 and 75.1%, respectively. Furthermore, the porosity increased with distance away from the cooled plate, regardless of the freezing temperature. While alkali solution was added into the slurry to keep the uniform distribution of ceramic particles, the sedimentation of ceramic particles occurred to certain extent, resulting in relatively higher solid loading of slurry on the bottom than that on the top. Therefore, the porosity of the bottom part with higher

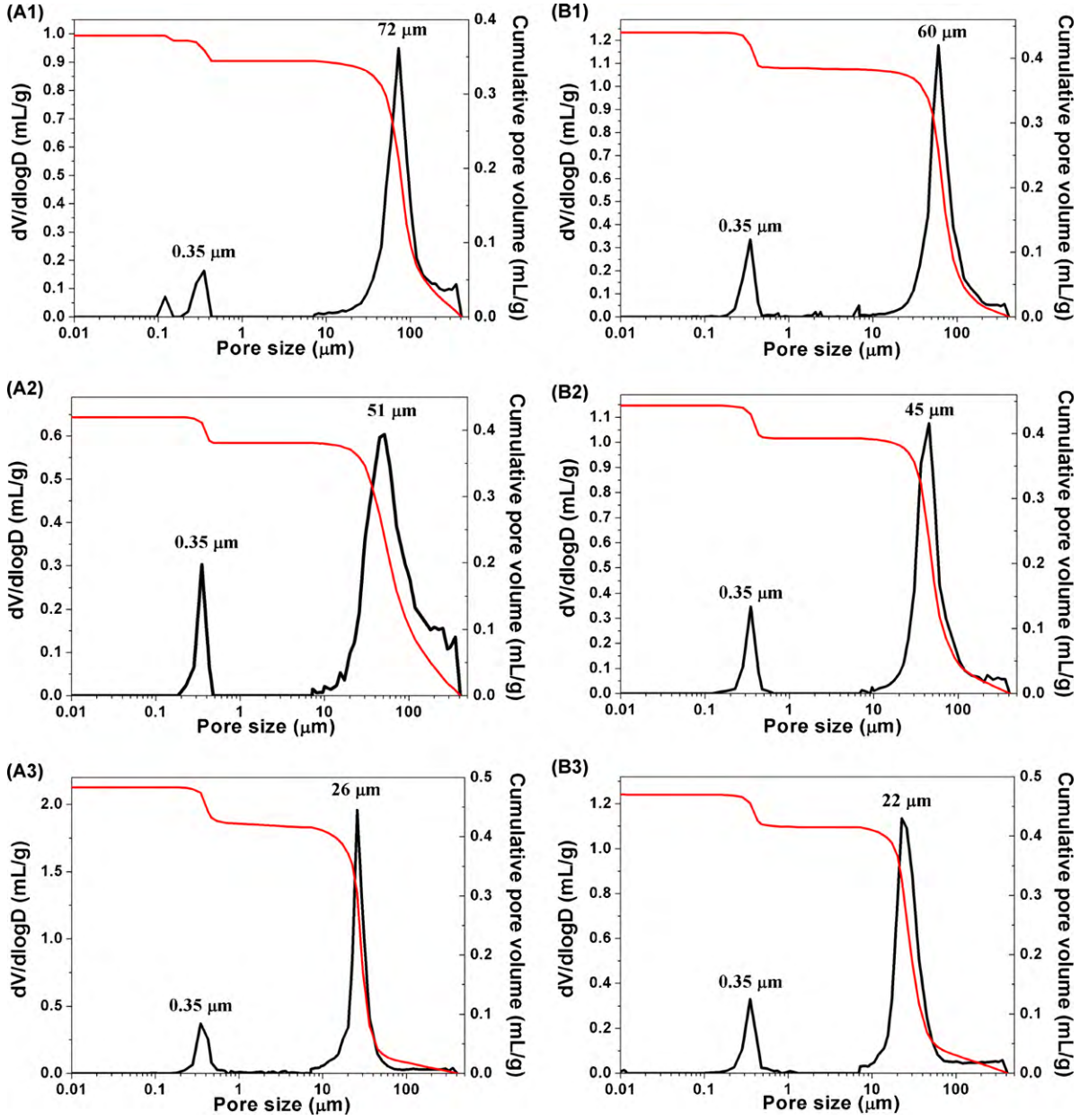

Fig. 5. Pore size distribution (bold line) and cumulative pore volume of porous YSZ ceramics at different locations from the cooled plate of 15 mm (A1, B1 and C1), 9 mm (A2, B2 and C2), 3 mm (A3, B3 and C3) and under different freezing temperatures of −30 °C (A1, A2 and A3), −78 °C (B1, B2 and B3) and −196 °C (C1, C2 and C3).

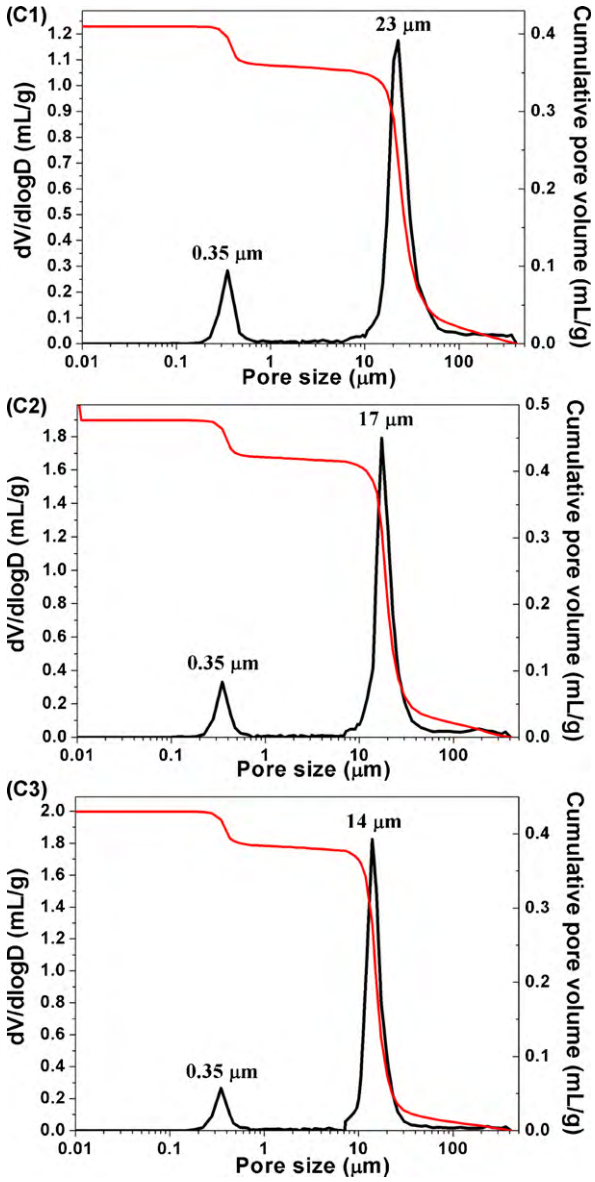

Fig. 5. (*Continued*)

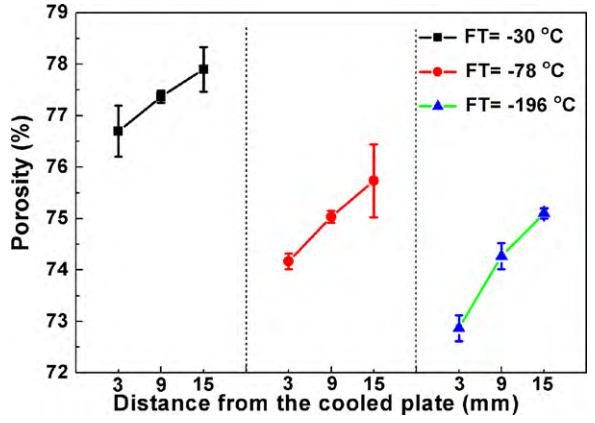

Fig. 6. Variation of porosity with distance from the cooled plate in porous YSZ ceramics with unidirectionally aligned pore channels under different freezing temperatures of −30, −78 and −196 °C.

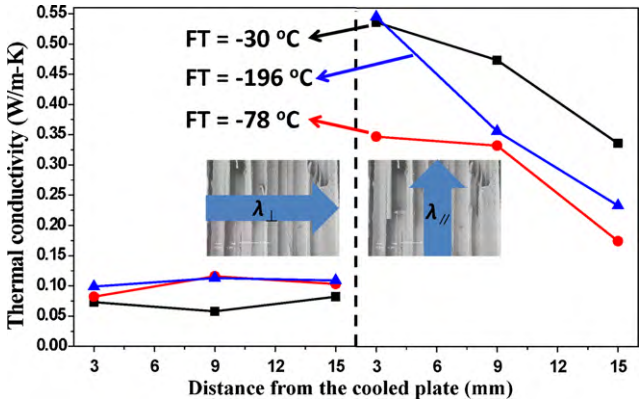

Fig. 7. Variation of room-temperature thermal conductivity with distance from the cooled plate of porous YSZ ceramics with unidirectionally aligned pore channels under different freezing temperatures of −30, −78 and −196 °C.

solid loading was lower than that of the top part with lower solid loading.

The decreasing solidification velocity in the freezing direction yielded porous YSZ ceramics with increasing pore channel size from 14 to 72 μm and increasing porosity from 73 to 78% in the two ends, respectively. Although it is important to keep the solidification velocity as constant as possible in order to obtain homogeneous materials, the structural characteristics in the porous YSZ ceramics brought advantages. For example, the end of porous YSZ ceramics with smaller pore channel size and porosity had potential applications in mechanical protection due to its higher strength; the end of porous YSZ ceramics with lager pore channel size and porosity performed better as thermal insulations due to its lower thermal conductivity.

3.4. Room-temperature thermal conductivity

Fig. 7 shows the variation of room-temperature thermal conductivity with distance from the cooled plate of porous YSZ ceramics with unidirectionally aligned pore channels under different freezing temperatures of −30, −78 and −196 °C. All the samples had low thermal conductivities, 0.06–0.36 W/m K, which were much lower than that of dense zirconia ceramics (∼2.18 W/m K). The porous YSZ ceramics are suitable for applications in thermal insulations. Notably, the thermal conductivity along the perpendicular direction ($\lambda_{\perp}$) was lower than that along the parallel direction ($\lambda_{//}$). The authors believed that the thermal conductivity along the perpendicular direction and the parallel direction could be modeled by series and parallel models for the structural characteristics, respectively. At a given porosity, the thermal conductivity predicted by the series model was lower than that predicted by the parallel model.[23] It was consistent with the experimental data. Although $\lambda_{\perp}$ were at the same level without considerable differences among different samples, $\lambda_{//}$ of sample under freezing temperature of −78 °C was lower than that of sample under freezing temperature of −30 and −196 °C. The reasons that $\lambda_{//}$ of sample under freezing temperature of −78 °C was the lowest were not clear.

4. Conclusions

In summary, this work reported the potential of using different freezing temperatures during freeze casting for controlling the pore channel size in porous YSZ ceramics with unidirectionally aligned pore channels for applications in thermal insulations. The pore channel size decreased significantly with decreasing freezing temperature, regardless of microstructure variations in the individual sample. Porosity also decreased as freezing temperature declined. While at a given freezing temperature, the pore channel size increased with increasing distance away from the cooled plate. Furthermore, the as-fabricated samples had remarkably low thermal conductivities ranging between 0.06 and 0.36 W/m K, and thus were suitable to be applied in thermal insulations.

Acknowledgement

This work was supported by the National Natural Science Foundation of China (Grant No: 90816019), the Natural High Technology Research and Development Program of China ("863" Program, Grant No: 2007AA03Z435) and State Key Development Program of Basic Research of China ("973" program, Grant No: 2006CB605207-2).

References

1. Ravichandran KS, An K, Dutton RE, Semiatin SL. Thermal conductivity of plasma-sprayed monolithic and multilayer coatings of alumina and yttria-stabilized zirconia. *J Am Ceram Soc* 1999;**82**: 673–82.
2. Garrido LB, Albano MP, Plucknett KP, Genova L. Effect of starch filler content and sintering temperature on the processing of porous 3Y-ZrO_2 ceramics. *J Mater Process Technol* 2009;**209**:590–8.
3. Sopyan I, Mel M, Ramesh S, Khalid KA. Porous hydroxyapatite for artificial bone applications. *Sci Technol Adv Mater* 2007;**8**:116–23.
4. Zhu XW, Jiang DL, Tan SH. Preparation of silicon carbide reticulated porous ceramics. *Mater Sci Eng A* 2002;**323**:232–8.
5. Falamaki C, Naimi M, Aghaie A. Dual behavior of Ca_2CO_3 as a porosifier and sintering aid in the manufacture of alumina membrane/catalyst supports. *J Eur Ceram Soc* 2004;**24**:3195–201.
6. Diaz A, Hamphshire S. Characterization of porous silicon nitride materials produced with starch. *J Eur Ceram Soc* 2004;**24**:413–9.
7. Zu LJ, Luo SJ. Study on the powder mixing and semi-solid extrusion forming process of SiCp/2024Al composites. *J Mater Process Technol* 2001;**114**:189–93.
8. Verdenelli M, Paarola S, Chassagneux F, Létoffé JM, Vincent HJ, Scharff P, Bouix J. Sol–gel preparation and thermor-mechanical properties of porous xAl_2O_3–$ySiO_2$ coatings on SiC Hi-Nicalon fibers. *J Eur Ceram Soc* 2003;**23**:1207–13.
9. Hu LF, Wang CA, Huang Y. Porous yttria-stabilized zirconia ceramics with ultra-low thermal conductivity. *J Mater Sci* 2010;**42**:3242–6.
10. Deville S, Saiz E, Tomsia AP. Freeze casting of hydroxyapatite scaffolds for bone tissue engineering. *Biomater* 2006;**27**:5480–9.
11. Deville S, Saiz E, Nalla RK, Tomsia AP. Freezing as a path to build complex composites. *Science* 2006;**311**:515–8.
12. Fukasawa T, Ando M, Ohji T, Kanzaki S. Synthesis of porous ceramics with complex pore structure by freeze-dry processing. *J Am Ceram Soc* 2001;**84**:230–2.
13. Fukasawa T, Deng ZY, Ando M. Synthesis of porous silicon nitride with unidirectionally aligned channels using freeze-drying process. *J Am Ceram Soc* 2002;**85**:2151–5.
14. Koh YH, Lee EJ, Yoon BH, Song JH, Kim HE. Effect of polystyrene addition on freeze casting of ceramic/camphene slurry for ultra-high porosity ceramics aligned pore channels. *J Am Ceram Soc* 2006;**89**:3646–53.
15. Han JC, Hong CQ, Zhang XH, Du JC, Zhang W. Highly porous ZrO_2 ceramics fabricated by a camphene-based freeze-casting route: microstructure and properties. *J Eur Ceram Soc* 2010;**30**:53–60.
16. Yoon HJ, Kim UD, Kim JH, Koh YH. Macroporous alumina ceramics with aligned microporous walls by unidirectionally freezing foamed aqueous ceramic suspensions. *J Am Ceram Soc* 2010;**93**:1580–2.
17. Hong C, Zhang X, Han J, Du J, Zhang W. Camphene-based freeze-cast ZrO_2 foam with high compressive strength. *Mater Chem Phys* 2010;**119**:359–62.
18. Zuo KH, Zen YH, Jiang D. Effect of polyvinyl alcohol additive on the pore structure and morphology of the freeze-cast hydroxyapatite ceramics. *Mater Sci Eng C* 2010;**30**:283–7.
19. Chen RF, Wang CA, Huang Y, Ma LG, Liu WY. Ceramics with special porous structures fabricated by freeze-gelcasting: using tert-butyl alcohol as a template. *J Am Ceram Soc* 2007;**90**:3478–84.
20. Oetting FL. The heat capacity and entropy of 2-methyl-2-propanol from 15 to 330 K. *J Phys Chem* 1963;**67**:2757–61.
21. Sciesinska E, Sciesinska J. Far infrared study of solid tert-butanol. *Acta Phys Pol A* 1980;**58**:361–8.
22. McGregor PA, Allan DR, Parsons S, Clark SJ. Hexamer formation in tertiary butyl alcohol (2-methyl-2-propanol, C4H10O). *Acta Crystallogr Sect B: Struct Sci* 2006;**B62**:599–605.
23. Carson JK, Lovatt SJ, Tanner DJ, Cleland AC. An analysis of the influence of material structure on the effective thermal conductivity of theoretical porous materials using finite element simulations. *Int J Refrig* 2003;**26**:873–80.